5.1.4 Magnetic Resonance Spectroscopy

Magnetic resonance spectroscopies are methods capable of detecting transitions of spin orientations of electrons or atomic nuclei between states separated energetically under the influence of an external magnetic field. Transitions involving the spin of the nucleus of an atom with a nonzero magnetic moment are studied with nuclear magnetic resonance spectroscopy (NMR), whereas transitions involving the spin of unpaired electrons in paramagnetic samples are investigated with electron spin resonance spectroscopy (ESR)[1]. Both methods are widely employed in analytical chemistry. NMR preferably of protons and ^{13}C-atoms and further selected atoms is presumably the most important method in analytical organic chemistry. ESR is used less frequently in studies of free radicals (chemical species with unpaired electrons) observed typically in organic reactions and in investigations of transition metal ions and paramagnetic substances.

Because in many electrochemical reactions, in particular in electroorganic ones, radicals are formed as reactive intermediates ESR has been applied frequently to studies of the mechanism and the kinetic of these reactions [5.1, 5.2 5.3]. Although possible, NMR spectroscopy has been used infrequently and only in very recent experiments mainly because of the considerably larger experimental effort [5.4]. With NMR spectroscopy information about surface structure, surface diffusion and electron spillover from the metal electrode onto an adsorbate can be obtained. So far an application as broad as that of ESR has not materialized. Both methods have been employed infrequently to monitor the concentration of species involved in electrochemical reactions in order to established reaction kinetic parameters, activation energies etc. These applications do not fall within the scope of this book, they are not considered here.

Fundamentals. Atoms are composed of nucleons: electrons, protons and neutrons (except the hydrogen atom, which has no neutron). These elementary particles have a spin, a property described in classical physics as a rotational movement of the particle around its own axis. It is a quantum property showing only certain quantisized values; for the electron the spin is $\boldsymbol{s}$ with the corresponding spin quantum number s = ½. The spin of an atomic nucleus $\boldsymbol{I}$ is composed of contributions of the nucleons. The corresponding angular momentum is $|\boldsymbol{s}| = \hbar/\sqrt{s(s+1)}$. This momentum is a vector, and its component parallel to a magnetic field H oriented in the z-direction can be $+\hbar/2$ or $-\hbar/2$. Because the proton and the electron are charged particles their rotation corresponds to a flow of electricity. This results in a magnetic momentum for the electron:

$$\boldsymbol{m}_s = g_e\, \gamma \boldsymbol{s} = \gamma_e \boldsymbol{s}$$

with g_e = electron g-factor, γ = magnetogyric ratio and γ_e = electron magnetogyric

[1] Frequently this method has been called electron paramagnetic resonance spectroscopy (EPR) because the presence of one or several unpaired electron being a precondition for this spectroscopy is also closely related to the phenomenon of paramagnetism.

ratio.

When considering an atom containing these nucleons in numbers characteristic for a given element, the resulting properties of the atom are slightly more complex. The resulting spin of the atomic nucleus depends upon the number of protons and neutrons and the relationship between both as listed in Table 5.x:

Table 5.x. Resulting nuclear spins as a function of protons and neutrons.

n_p	n_n	resulting nuclear spin $\boldsymbol{I}$	example
odd	odd	integer number	^{2}H, ^{14}N, ^{10}B
odd	even	half-number value	H, ^{13}C, ^{15}N, ^{19}F, ^{31}P, ^{11}B, ^{29}Si
even	odd	half-number value	see above
even	even	zero	^{12}C, ^{16}O, ^{28}Si, ^{30}Si

The value of the magnetic momentum $\boldsymbol{m}_l$ for the atomic nucleus is

$$\boldsymbol{m}_l = g_N \gamma \boldsymbol{I} = \gamma_N \boldsymbol{I}$$

with g_N = nuclear g-factor and γ_N = nuclear magnetogyric ratio.

In atoms or molecules containing several electrons only unpaired electrons present in singly occupied atomic or molecular orbitals show an effective magnetic momentum.

The vectors representing the nuclear or the electron angular momentum and the associated magnetic momentum of particles in a given sample are randomly orientated. This is changed drastically when the sample is exposed to an external magnetic field. Because of the interaction between the magnetic field and the magnetic momentum of the electron or the atomic nucleus the momentum is oriented in one of two possible directions relative to the external field vector. The momentum is not oriented exactly parallel to the field vector; consequently the vector shows a precession movement with a characteristic Larmor frequency. A calculation of the potential energy of the species in the magnetic field is based on the size of the vectorial component of the magnetic moment in the z-direction. This is given for an electron by

$$|\boldsymbol{m}_{sz}| = |- g_e \mu_B m_s|$$

with μ_B = Bohr magneton.

The corresponding value for a nucleus is

$$|\boldsymbol{m}_{lz}| = | g_N \mu_N m_N |$$

with μ_N = nuclear Bohr magneton.

The potential magnetic energy E for a dipole $\boldsymbol{m}_z$ in a magnetic field is

$$E = - \boldsymbol{m}_z \boldsymbol{B}.$$

With the electron the result is

$$E = g_e \, \mu_B \, m_s \, \boldsymbol{B},$$

for the nucleus it is

$$E = - g_N \, \mu_N \, m_l \boldsymbol{B}.$$

For a proton with $m_N = ½$ only two orientations corresponding to $m_l = ½$ and $m_l = -½$ are possible, this case will be considered as an example for NMR subsequently. Of course other nuclei with $m_N > ½$ posess more than only two nondegenerate energy levels. They are spaced equally, this implies that only one resonant transition is observed.

For both the electron and the nuclear momentum the calculated energy depends upon the actual orientation of the momentum vector. The values energetically lower are those corresponding to $m_s = -½$ and $m_l = +½$. Energies for the electron are larger by three orders of magnitude. The actual energies and the differences between various orientations depend upon the magnitude of the magnetic field. A calculation of the difference is possible assuming a temperature of e.g. 300 K and a magnetic flux density of $B = 0.3$ T for investigations of the electron spin and $B = 1.409$ T for those of the nuclear (in this example the proton) spin. Results are:

$$\Delta E_s = g_e \, \mu_B \, B = 5.57 \cdot 10^{-24} \text{ J}$$

and

$$\Delta E_N = g_N \, \mu_N \, B = 3.97 \cdot 10^{-26} \text{ J}.$$

The differences in population between the corresponding states can be calculated assuming a Boltzmann distribution. For the electron spin the ratio $n_{s,high}/n_{s,low} = 0.99866$, for the proton $n_{N,high}/n_{N,low} = 0.99999039$. A transition of the orientational state of the spins from the lower into the higher state is possible only if the necessary energy is supplied under resonant conditions to the system. Continuous absorption of this specific energy occurs only, when there is a smaller population of the higher energy level. This in turn depends upon relaxation of system from the higher state into the lower one which is possible only, when effective ways of dissipating the energy exist. Spontaneous emission, which provides an effective path of depopulating higher levels in optical spectroscopies, is extremely low and can be neglected. Consequently stimulated emission initiated by the incoming radiation and interactions with other particles (spin-spin relaxation) and the surrounding matter (spin-lattice relaxation) provide the required energy dissipation. Since the difference in energies between both states of orientation depends upon the strength of the magnetic field B the resonance condition is described properly by stating both B and the frequency of the electromagnetic radiation. For a proton in a magnetic field with a flux density of $B = 1.409$ T the frequency is $60 \cdot 10^9 \text{ s}^{-1}$, at a stronger magnetic flux density of $B = 11.74$ T employed in advanced spectrometers resonance occurs at $500 \cdot 10^6 \text{ s}^{-1}$. For an electron in a field of $B = 0.34$ T the

value is $9.5 \cdot 10^9$ s^{-1}.

The previous discussion assumes, that both the unpaired electron(s) and the atomic nuclei interact soleley with the magnetic field. Correspondingly the resonance condition should be fixed as described. In reality both are surrounded by other species influencing the effective magnetic field at the location of the electron or nucleus by means of their own electric and magnetic properties. Based on the type of chemical bond and the electronegativity of the participating elements the electron density at the atom under investigation can change considerably. In the case of the nucleus the resulting effect is particularly pronounced. The actual resonance condition is changed accordingly. Appropriately this is called a chemical shift, because of its high specificity it can be used as a tool in identification of the molecular structure. The influence upon the unpaired electrons is much smaller and of only very limited analytical value. Besides this effect related to the local electron density the magnetic spins of neighbouring atoms can influence the local field. Depending upon the relative orientation the field is increased or decreased, again the resonance condition is changed. Because of the number of combinations of orientations of magnetic spins in a multi-atom system several additional resonant transitions may occur. The effect is termed hyperfine splitting with ESR; in NMR it is called spin-spin-splitting because it is the result of an interaction of nuclear spins. In solid samples anisotropic effects of electrostatic or magnetic fields caused by the atomic or molecular constituents of the sample and their particular arrangement can also change the effective magnetic field resulting in both shifts and splitting. This effect is not present in liquid and gaseous samples. With both spectroscopies the number of additional lines, their relative intensities and energetic difference provide valuable information for the elucidation of the molecular structure. In electrochemical applications discussed below in more detail electron spin resonance is used more often, thus some example shall illustrate the brief outline of magnetic resonance spectroscopies. The number N of lines created by n nuclei labelled k of spin $\boldsymbol{I}_k$ is

$$N = \prod_k (2n_k \, \boldsymbol{I}_k + 1).$$

The distance of the lines corresponding to the energetic difference is stated by giving a splitting constant a (sometimes also named coupling constant). The relative intensity of the lines depends upon the probability of transitions between the states involved; this in turn depends on the probability of the various combinations of orientations. In Fig. 5.X the calculated ESR spectrum of the methyl radical is depicted.

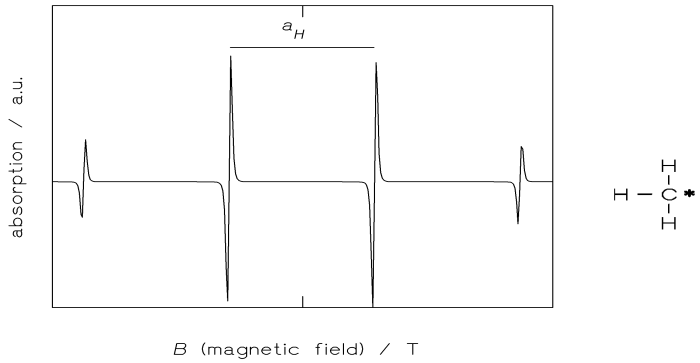

Fig. 5.X. Calculated ESR absorption spectrum of the methyl radical

As in ESR spectra for reasons caused by the mode of detection of the absorption signal (see below) always the first derivative is measured, the simulated spectra shown here are plotted accordingly. With a spin $\boldsymbol{I}_H = ½$ and $n = 3$ the number N of lines is four. With a considerably more complex molecule di-tert-butylnitroxid in its radical form a surprisingly simple spectrum as shown in Fig. 5.X results. We can understood it easily when taking into account, that the free electron is located at the nitrogen atom ($\boldsymbol{I} = 1$), whereas both oxygen and carbon have $\boldsymbol{I} = 0$ (see above).

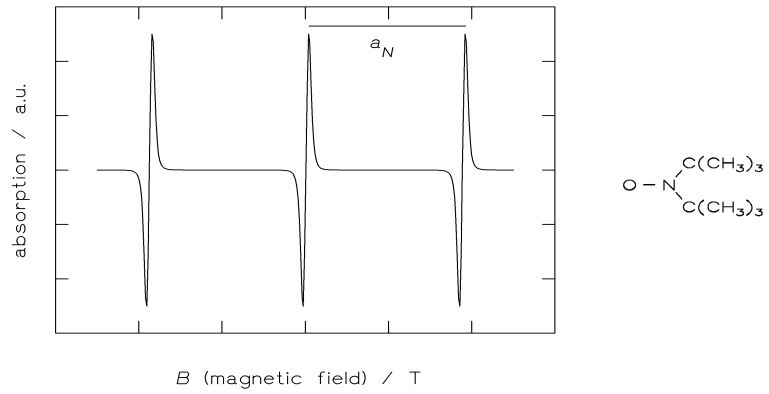

Fig. 5.X. Calculated ESR absorption spectrum of the di-tert-butylnitroxid radical

A check for the correctness of a simulated spectrum is provided by comparing calculated and measured spectra. In Fig. 5.X the measured and the calculated spectra of the electrochemically generated nitropropane radical are shown.

Upon the rather wide splitting caused by the nitrogen atom a further splitting caused by the two methylene hydrogen atoms at the carbon atom next to the nitrogen is superimposed. The hydrogen atoms at the vicinal methyl group are too far away, they do not cause any further splitting. Further details are discussed in textbooks of magnetic resonance spectroscopy (see suggested reading).

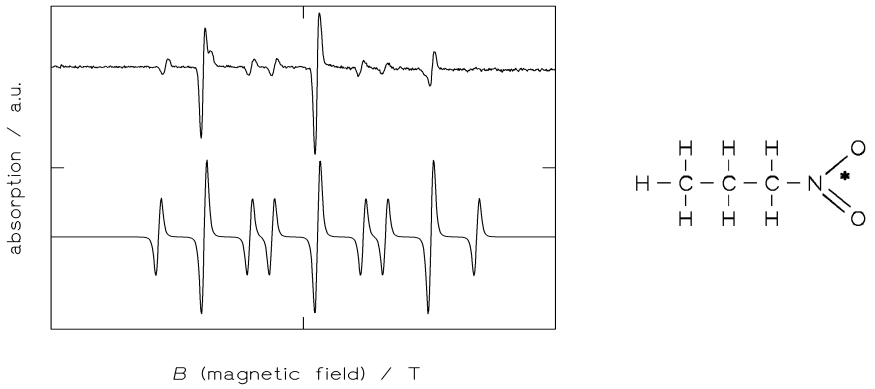

Fig. 5.X. ESR absorption spectrum of the electrochemically generated nitropropane radical anion; E_{NHE} = – 1740 mV; top: measured spectrum, bottom: calculated spectrum; hyperfine splitting constants a_N = 2.48 mT, a_H = 0.998 mT

Instrumentation. From the description of the fundamentals of magnetic resonance spectroscopy basic building blocks and functional elements of the experimental can be derived easily: The sample has to be brought into a magnetic field of appropriate strength. The energy corresponding to the difference between the two states of the nuclear or electron spin is supplied as electromagnetic radiation of suitable frequency, generally in the radio-frequency range or, more precisely, in the micro-wave range for ESR and in the UHF-range for NMR[1]. Because of the modes of propagation of radiation in the micro-wave range waveguides have to be used instead of cables. The sample is inserted into a cavity at the end of a waveguide in between the poles of the magnet. Since the actual resonance conditions are shifted from the reference values stated above either the strength of the magnetic field (i.e. the magnetic flux) or the radiation frequency has to be tuned in order to detect the actual resonance. A modulation of the frequency of the radiation supplied at constant intensity (cw: continuous wave) with the necessary precision and stability is somewhat difficult to obtain for reasons related to high frequency electronics. A direct modulation of the magnetic field by simply changing the current flowing across the coils of the electromagnets employed frequently in NMR and practically exclusively in ESR is cumbersome because of the need to control pretty large electric currents. In the case of very strong magnets using superconducting coils this is impossible anyway. A more effective approach is the addition of small additional coils attached to the poles of the main magnet. The additional magnetic flux provided by these modulation coils can be controlled easily. Consequently the resonance conditions are probed by changing the magnetic field slowly. Absorption of electromagnetic radiation can be detected by various means. The actual absorption in particular with ESR is rather small because of the small difference in occupation of both states. An increase of sensitivity can be obtained by applying sophisticated amplification and detection methods

[1] UHF: ultra high frequency

(phase sensitive detection with lock-in amplifiers). In the case of ESR this results in spectra being equivalent to the first derivative of the actual absorption spectrum. More recently the Fourier Transform (FT) technique already described in Sect. 5.1.2 as applied to vibrational spectroscopy has been adapted for ESR and NMR. The electromagnetic radiation is supplied as a pulse. Detection and data manipulation is more complex, the advantage is a greatly enhanced sensitivity. This is described in more detail in textbooks of spectroscopy.

Basically an NMR or ESR spectrometer is composed of a magnet, a radio frequency generator, an additional generator driving the field modulation coils, and the necessary detector and data manipulation and storage electronics. The sample is inserted into the magnet between its poles. Some preparation of the sample is generally necessary, materials containing ESR- or NMR-active substances have to be avoided as sample holder. Various types of cuvets for solid, liquid and gaseous samples are in use. In NMR spectroscopy almost exclusively quartz tubes of various diameters free of paramagnetic impurities are used. In ESR spectroscopy different shapes (tubes, flat cells) of cuvets are used depending upon the type of cavity (cyclindrical ones for the former, rectangular ones for the latter cuvets).

For electrochemical applications the experimental arrangement is rather simple. Because of the broad application of ESR this method is treated first, some additional information on NMR in electrochemistry can be found at the end of this chapter. In ESR experiments the spectrum can be recorded with the species under investigation created just inside the spectrometer (intra muros generation, subsequently treated as *in situ* method) or outside the spectrometer (extra muros). In the latter case the sample has to be transferred by means of a flow apparatus or by removal of a small sample from the electrochemical cell, which is put into a standard ESR cuvet. For reasons alreaday outlined in chapter 4 the latter procedure being similar to an *ex situ* experiment carries some inherent sources of error because of e.g. limited lifetime or subsequent chemical reactions of the species initially created by the electrochemical reaction. Since with respect to the ESR spectrometer no particular design of the cuvet is necessary the latter procedure will not be discussed in detail.

Generation of species and their detection inside the cavity of the ESR spectrometer need some consideration of experimental requirements of the spectrometer and an appropriate electrochemical cell design. Since most electrochemical reactions proceed at metal electrodes a very fundamental problem is encountered in any attempt to obtain ESR spectra of radicals still adsorbed, i.e. interacting strongly, on the electrode surface. This interaction between the unpaired electron of the radical and the electrons in the metallic conductor will quench the free spin; no ESR spectrum will be observed. This is different with semiconductor or insulator electrode surfaces. The quenching can be suppressed by coating the electrode with a layer of nonmetallic material (chemically modified electrode), but obviously this may change the interesting properties of the electrode considerably. Nevertheless ESR-active species can be detected as soon as they leave the electrode surface and stay in the electrolyte solution at a sufficiently large concentration for a time long enough in order to allow measuring a spectrum. The first requirements seems somewhat odd at first glance, because ESR is a rather sensitive spectroscopy. Paramagnetic species at a concentration as low as 10^{-10} mol dm^{-3} can be detected easily. Unfortunately the high reactivity of organic radicals

tend to keep the stationary concentration low, in addition the components of the electrochemical cell (electrolyte, solvent, electrodes) reduce the sensitivity of the spectrometer considerably in particular by increasing dielectric losses. Detection of radicals being present in only very small concentrations or of short lifetime can be facilitated by using „spin traps“. These are mostly organic compounds which form stable radicals by reaction with the radicals formed during the investigated process. In many cases these spin traps contain a nitroso group. The observed ESR spectra are more or less complicated depending on the type of spin trap and the trapped radical. A fairly simple spectrum is obtained by using *t*-nitroso-butane NtB as a spin trap (for further details see below). The adduct formed with hydrogen radicals causes the spectrum depicted in Fig. 5.X, for further details see below..

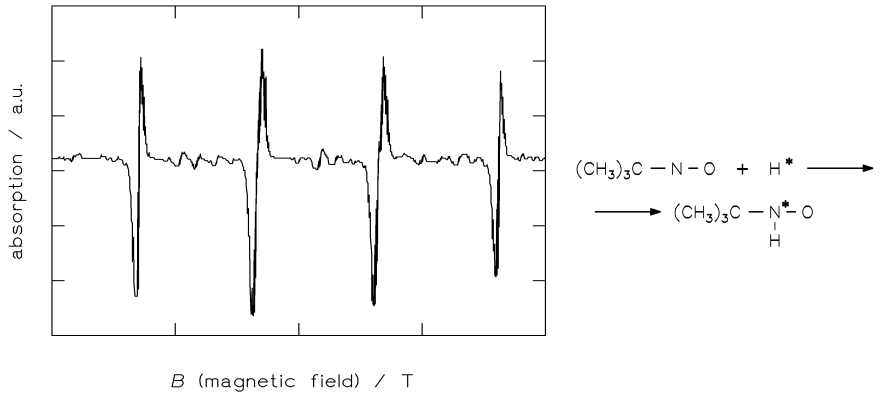

Fig. 5X. ESR spectrum of the hydrogen-adduct of NtB generated electrochemically at E_{SCE} = 0.2 V in an aqueous solution of 0.5 **M** $LiClO_4$ [5.5]

A first cell design with two electrodes was reported by Maki and Geske [5.6] (Fig. 5.X). A platinum wire used as a working electrode was mounted in the center of a quartz tube serving as a cell vessel in the middle of the ESR-cavity at the position of highest sensitivity. A platinum wire as the counter electrode was mounted in the tube at a position outside the cavity of the spectrometer. Any species created at this counter electrode will not be detected; in addition the distance between both electrodes reduces the risk of unwanted electrochemical reactions at the working electrode of species created at the counter electrode. The small actual surface area of the working electrode limited the rate of formation of species to be studied, very precise positioning was required. Because of the simple design nevertheless this cell design has been used continuously despite the obvious drawbacks and limitations [5.7]. Using a vanadium wire as working electrode VO^{2+} ions could be identified as electrooxidation products [5.8].

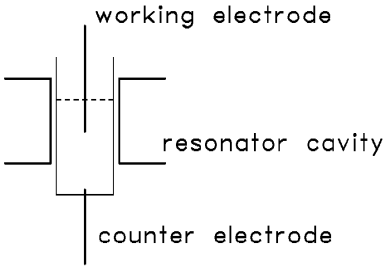

Fig. 5.X. Cell design for ECESR spectroscopy according to Maki and Geske [5.6].

An increase of the surface area was realized by Piette et al. [5.9] (Fig. 5.x). A platinum gauze electrode was put inside a flat cuvet used as the electrochemical cell. The counter electrode was mounted inside a glass tube attached to the flat cell below the working electrode and outside the ESR cavity.

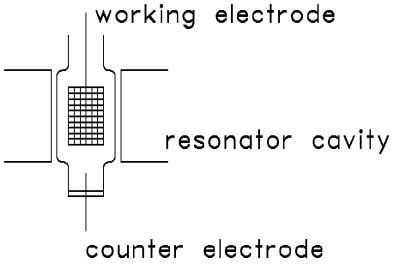

Fig. 5.X. Cell design for ECESR spectroscopy according to Piette et al. [5.9]

A cell of this design was employed in studies of microcrystal solids attached to a platinum flag electrode [5.10]. The measured ESR-spectrum of electrochemically reduced 7,7',8,8'-tetracyanoquinodimethane was in perfect agreement with the respective spectrum of the chemically prepared compound as well as the simulated spectrum.

A cell design suitable for investigations with a mercury electrode was described by Möbius [5.11] (Fig. 5.x).

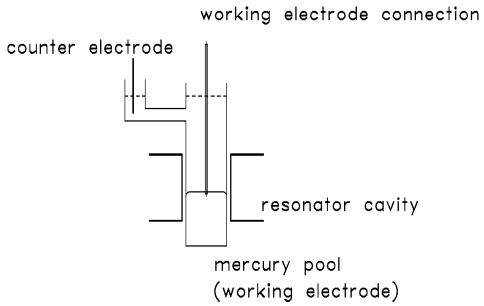

Fig. 5.X: Cell design for ECESR spectroscopy according to Möbius [5.11].

Unfortunately these two-electrode cell designs did not allow for proper control of the electrode potential of the working electrode. In a modified design Piette et

al. [5.12] added a reference electrode connected to the electrolyte volume via the glass tube on top of the flat cell (Fig. 5.x).

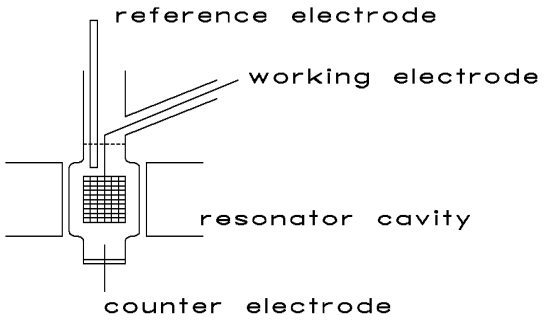

Fig. 5.X. Cell design for ECESR spectroscopy according to Piette et al. [5.12]

This design has been employed to study the electrochemistry of microdroplets attached to an electrode in contact with an electrolyte solution [5.13]. A microdroplet of *N*,*N*,*N*',*N*'-tetrahexylphenylene diamine deposited onto a gold electrode immersed into an aqueous electrolyte solution showed only a symmetric single line ESR signal similar to those observed with intrinsically conducting polymers. In a dilute solution of the same moleculae in a suitable organic solvent a well resolved spectrum showing the expected hyperfine structure was observed.

A design similar to that of Piette et al. was reported by Koopman and Gerischer [5.14] (Fig. 5.x).

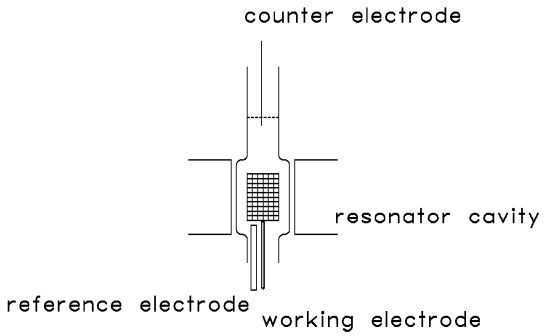

Fig. 5.X. Cell design for ECESR spectroscopy according to Koopman and Gerischer [5.14]

A significantly more simple cell design with a smaller working electrode surface and consequently smaller currents flowing through the cell in the case of potentiostatically controlled measurements has been reported by Bagchi et al. [5.15]. A capillary tube housing a platinum wire acting as a reference electrode fits into a modified cuvet placed in the microwave cavity of the ESR spectrometer thus displacing most of the electrolyte solution in the lower part of the cell exposed to the microwave. Accordingly solvents with high dielectric constants can be used with a satisfactory ESR response. The platinum wire sealed into the bottom of the Pyrex cuvet acting as the working electrode can be coated easily with a drop of mercury

for experiments where this type of electrode is required. The Pyrex glass may cause unwanted ESR signals; unfortunately platinum cannot be sealed directly to quartz glass.

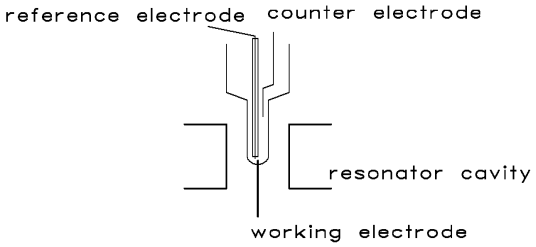

Fig. 5.X. Design of an ECESR cell proposed by Bagchi et al. [5.15]

Mu and Kadish have described an ECESR cell with a thin layer design suitable for measurements at both ambient and low temperatures [5.16]. The thin layer of electrolyte solution is enclosed by the quartz tube inserted into the microwave cavity of the ESR spectrometer and a solid quartz rod fixed in the center of the tube. An expanded platinum mesh in the gap is used as the working electrode. At low electrode potential scan rates the cell shows an acceptable electrochemical response.

A mechanically robust ECESR cell suitable for measurements even at very low temperatures with all kinds of electrolyte solvents employing a platinum wire loop as working located at the bottom of a 4 mm ESR cuvet has been developed by Fiedler et al. [5.17]. Reference and counter electrode are placed above the working electrode outside of the sensitive region of the ESR cavity.

The very small electrolyte volume present inside the flat cell poses a serious problem, because the concentration of the reacting species is rapidly diminished upon continuous flow of a Faradaic current. In the latter design this was corrected by a slow upward flow of electrolyte solution through the cell. A very similar setup was described by Dohrmann and Vetter [5.18].

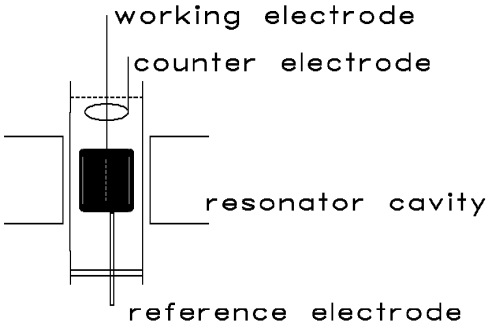

Fig. 5.X. Cell design for ECESR spectroscopy according to Dohrmann and Vetter [5.18]

The fairly long solution pathways in the three-electrode cell designs caused a poor dynamic response of the cell under instationary conditions; the electrode potential control was imperfect. A flat cell design by Goldberg and Bard [5.19] provided considerable improvement. The limited amount of electrolyte solution re-

sulted in fast depletion of reactand.

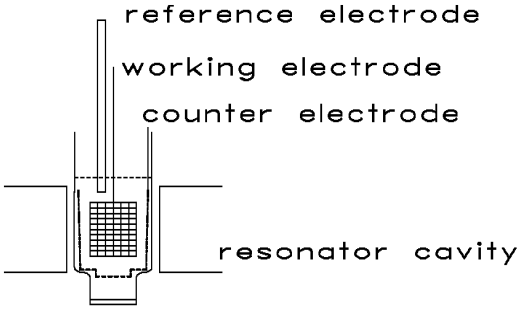

Fig. 5.X. Cell design for ECESR spectroscopy according to Goldberg and Bard [5.19]

A considerable improvement in terms of electrode potential distribution inside the ECESR cell, availbale electrolyte solution volume and ease of manufacturing was provided with the cell design of Allendoerfer et al. [5.20] subsequently improved by Heinzel et al. [5.5, 5.21]. A metal wire coil of the working electrode material is inserted into a quarz glass tube. Because of the limited penetration depth of the microwaves onle the solution volume enclosed by the wire surface and the inner glass wall is probed. The counter and the reference electrode inserted centrally inside the working electrode coil can be made without major constraints caused by cell or working electrode design. Because of the size of the cell a less common large cylindrical microwave cavity is required. The cell components are shown in detail in Fig. 5.x.

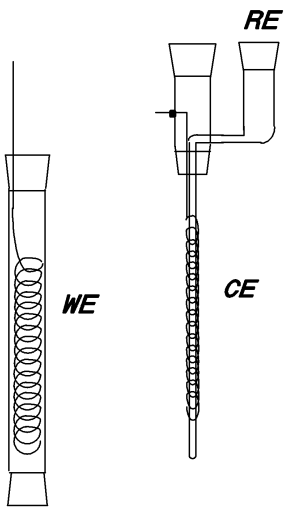

Fig. 5.X. The components of an ECESR cell according to Heinzel et al. [5.5]

The superior electrochemical performance of this design is demonstrated with a cyclic voltammogram as shown Fig. 5.X.

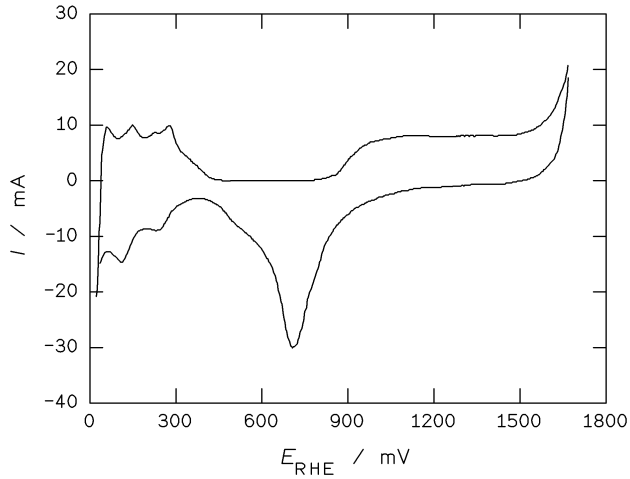

Fig. 5.X. Cyclic voltammogram of a platinum wire working electrode inside an ECESR cell according to Heinzel et al.; electrolyte solution 1 **N** H_2SO_4, dE/dt = 50 mV s^{-1}; nitrogen purged [5.22]

The cell has been employed in studies of electrooxidation of organic fuels [5.5, 5.21, 5.23] and of nitrogen-containing monomers for the generation of intrinsically conducting polymers [5.24, 5.25, 5.26]. In numerous studies films of intrinsically conducting polymers deposited onto the working electrode have been investigated [5.27, 5.28, 5.29]. Because of the high degree of delocalization the radical cations created by oxidation (*p*-doping) of the film show only a single line. The amplitude of the signal corresponds to the concentration of free spins and thus presumably to the number of mobile charge carrier. In a plot of ESR spectra obtained as a function of electrode potential this can be illustrated (Fig. 5.???). The striking similarity, which in some cases even extends to small asymmetries in line shape, has caused early erroneous asisgments of the line as being caused by mobile electrons as observed with ESR in case of metals by Dyson (Dysonian line, [5.30]).

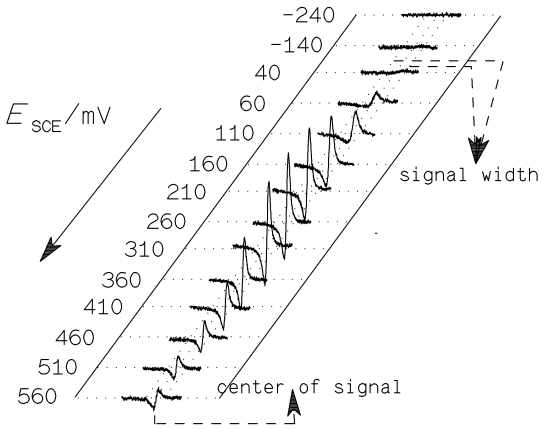

Fig. 5.X. ESR spectra of a film of polyaniline in a solution of 0.1 **M** $LiClO_4$ in acetonitrile

The major drawbacks of cells as described above with stationary solutions or very low solution flow are the limited supply of reactand and consequently a limited maximum concentration of species to be studied. Various designs of flow-through cells have been proposed. A review by Bagchi et al. [5.31] describes selected examples. Since it has been shown that the stationary concentration of the species to be detected decreases with an increasing flow rate [5.32] the actual operating conditions have to be optimized individually. A cell design as proposed by Bagchi et al. [5.15] is shown in Fig. 5.X.

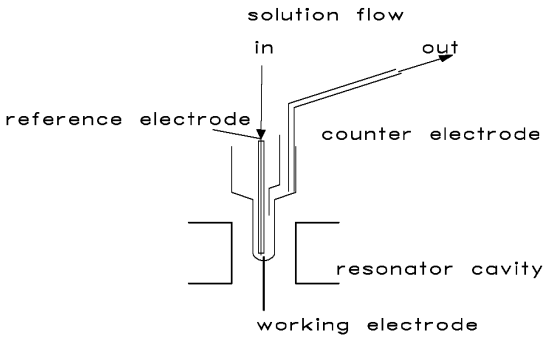

Fig. 5.X. Design of a flow-through ECESR cell proposed by Bagchi et al. [5.15]

An optimized design employing a tubular electrode in a cylindrical cavity has been described [5.33]. A similar design suitable for low temperature measurements (233 K) has been reported [5.34]. It has been employed in a study of the temperature dependence of the reduction of bromonitrobenzene in acetonitrile solution. The electroreduction of perinaphthenone in a single electron process has been investigated with this cell [5.35]. The lifetime of the neutral radical formed by deprotonation of the radical anion has been estimated to be around 1 min. A similar

electrochemical behavior of benzanthrone was observed.

A combination if ECESR and *in situ* UV-vis spectroscopy has been proposed by Petr et al. [5.36]. In a cell designed similar to the ECESR cell proposed by Piette [5.9] a UV-vis spectrometer is coupled to the cell via fiber optics. The working electrode is of a minigrid type. A cell design with an electrochemical cell directly coupled to a cuvet fitting into the ESR spectrometer has been described by Friedrich and Baumgarten [5.37].

Although the detection limit for ESR spectroscopy per se is extremely low the use of electrochemical cells filled with solvents of high dielectric constants results in considerable losses in the cavity of the ESR spectrometer. This in turn increases the limit of detection. In the case of electrode reactions having only very small stationary concentrations of radicalic intermediates their detection may be impossible. The use of spin traps may help. These compounds are rather simple organic molecules reacting easily with radicals forming adducts (see Fig. 5.x). From the known structure of the spin trap and the observed ECESR spectrum the molecular structure of the intermediate may be deduced. Unfortunately this technique tends to trap not necessarily the major reaction intermediate, but only those which react easily with the spin trap. Consequently misinterpretations are possible.

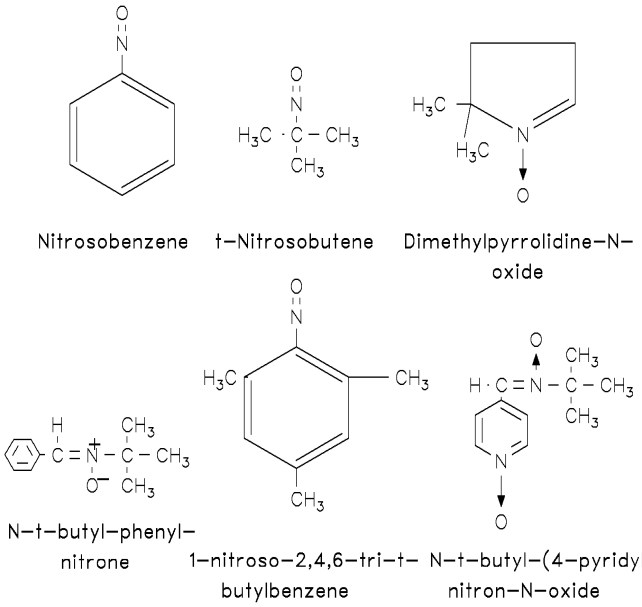

Fig. 5.X: Examples of organic compounds used as spin traps in ECESR spectroscopy.

Cell designs for *in situ* NMR spectroscopy with electrochemical cells are scant. Because of the low sensitivity designs with working electrodes having large active surface areas (powder electrodes, metal coated inert supports like e.g. silica or alumina) have been described [5.38, 5.39]. This is a result of the fact, that in a typical NMR experiment about 10^{19} spins are required. Assuming 10^{15} surface at-

oms on 1 cm^2 metal surface area at complete coverage of all adsorption sites 1 m^2 working electrode surface area is required. A typical design is shown in a schematic drawing in Fig. 5.X. If continuous electrode potential during aquisition of the NMR spectrum is desired particular attention has to be paid to proper shielding and decoupling of the electrical wiring between potentiostat and NMR probe head.

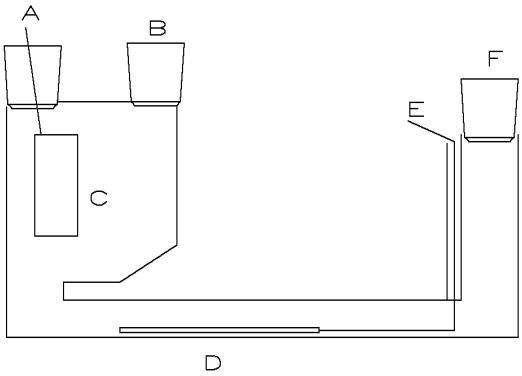

Fig. 5.X. Schematic drawing of an electrochemical cell for in situ NMR spectroscopy [5.38]. A counter electrode connection, B reference electrode joint, C counter electrode, D platinum black working electrode, E working electrode connection, F purge connection

Results reported so far pertain in particular to ^{13}C-NMR spectroscopy of adsorbed CO and CN^--ions on platinum [5.38, 5.40]. Besides information about surface diffusion and electronic adsorbate-surface interaction data on the effect of the strong electric field at the electrochemical interface (typically 10^7 V cm^{-1}) have been reported. With both adsorbates the ^{13}C-resonance becomes more shielded at more positive electrode potentials as expected when assuming an adsorbate attachment via the carbon atom. These results were supported with data from ^{195}Pt-NMR spectroscopy [5.41]. Differences in the electrooxidation of methanol and CO on carbon-supported platinum hasve been associated with different linewidths of the ^{13}C-signal [5.42].

The use of NMR spectroscopies with various species like e.g. H, F, Na, Al or Li in studies of solid electrolytes has been reviewed elsewhere [5.43].

Further reading:

On ESR-spectroscopy:

R. Kirmse and J. Stach: ESR-Spektroskopie, Akademie-Verlag, Berlin 1985

J.E. Wertz and J.R. Bolton: Electron Spin Resonance, Chapman & Hall, New York 1986

N.M. Atherton: Principles of Electron Spin Resonance, Ellis Horwood PTR Prentice Hall, Chichester 1993

K. Scheffler, H.B. Stegmann: Elektronenspinresonanz, Springer-Verlag, Berlin 1970

C.P. Poole, Jr.: Electron Spin Resonance, Dover Publications Inc., Mineola 1996

C.P. Poole and H.A. Farach: Handbook of electron spin resonance 1, AIP Press 1997

C.P. Poole and H.A. Farach: Handbook of electron spin resonance 2, Springer Verlag 1999

On NMR-spectroscopy:
J.W. Akitt: NMR and Chemistry, Chapman&Hall, New York 1983
E.D. Becker: High Resolution NMR, Academic Press, New York 1980
F.A. Bovey: Nuclear Magnetic Resonance Spectroscopy, Academic Press, New York 1988
R.K. Harris: Nuclear Magnetic Resonance Spectroscopy, Longman Scientific& Technical, Essex 1986

References

5.1 R.G. Compton and A.M. Waller: Spectroelectrochemistry (R.J. Gale Ed.), Plenum Press, New York 1988, p. 349.

5.2 T.M. McKinney in: Electroanalytical Chemistry Vol. **19** (A.J. Bard Eds.), Marcel Dekker, New York 1996, p. 109.

5.3 R. Holze, Recent Res. Devel. Electrochem. **6** (2003) 111.

5.4 A. Wieckowski, Extended Abstracts of the 203rd Meeting of the Electrochemical Society, Paris, France, 27.04.-02.05.2003, Ext.Abstr.1249.

5.5 A. Heinzel, PhD-Dissertation, Universität Oldenburg 1985.

5.6 A.H. Maki andD.H. Geske, Anal. Chem. **31** (1959) 1450; J. Chem. Phys. **30** (1959) 1356; **33** (1960) 825;
D.H. Geske and A.H. Maki, J. Am. Chem. Soc. **82** (1960) 2671; **83** (1961) 1852.

5.7 W. Kaim, S. Ernst, and V. Kasack, J. Am. Chem. Soc. **112** (1990) 173.

5.8 M.A.M. Ameer and A.A. Ghoneam, J. Electrochem. Soc. **142** (1995) 4082.

5.9 L.H. Piette, R. Ludwig, and R.N. Adams, J. Am. Chem. Soc. **83** (1961) 3909; **84** (1962) 4212.

5.10 A.M. Bond and D.A. Fiedler, J. Electrochem. Soc. **144** (1997) 1566.

5.11 K. Möbius, Z. Naturf. **20A** (1965) 1093; Angew. Physik **17** (1964) 534.

5.12 L.H. Piette, R. Ludwig, and R.N. Adams, Anal. Chem. **34** (1962) 916; **34** (1962) 1587.

5.13 F. Marken, R.D. Webster, S.D. Bull, and S.G. Davies, J. Electroanal. Chem. **437** (1997) 209.

5.14 R. Koopman and H. Gerischer, Ber. Bunsenges. Phys. Chem. **70** (1966) 118.

5.15 R.N. Bagchi, A.M. Bond, and F. Scholz, J. Electroanal. Chem. **252** (1988) 259.

5.16 X.H. Mu and K.M. Kadish, Electroanalysis **2** (1990) 15.

5.17 D.A. Fiedler, M. Koppenol, and A.M. Bond, J. Electrochem. Soc. **142** (1995) 862.

5.18 J.K. Dohrmann and K.J. Vetter, J. Electroanal. Chem. **20** (1969) 23;
J.K. Dohrmann, Ber. Bunsenges. Phys. Chem. **74** (1970) 575;
J.K. Dohrmann and F. Galluser, Ber. Bunsenges. Phys. Chem. **75** (1971) 432;
J.K. Dohrmann, F. Galluser, and H. Wittchen, Faraday Discuss. Chem. Soc. **56** (1973) 350.

5.19 I.B. Goldberg and A.J. Bard, J. Phys. Chem. **75** (1971) 3281.

5.20 R.D. Allendoerfer, G.A. Martincheck, and S. Bruckenstein, Anal. Chem. **47** (1975) 890;
R.D. Allendoerfer, J. Am. Chem. Soc. **97** (1975) 218.

5.21 A. Heinzel, R. Holze, C.H. Hamann, J.K. Blum, Z. Phys. Chem. NF **160** (1989) 11.

5.22 R. Holze, Habilitation thesis, Universität Oldenburg 1989.

5.23 A. Heinzel, R. Holze, C.H. Hamann, and J.K. Blum, Electrochim. Acta **34** (1989) 657.

5.24 C.H. Hamann, R. Holze, and F. Köleli, DECHEMA-Monographie **121** (1990) 297.
5.25 R. Holze, F. Köleli, and C.H. Hamann, DECHEMA-Monographie **117** (1989) 315.
5.26 R. Holze and C.H. Hamann, Tetrahedron **47** (1991) 737.
5.27 J. Lippe, PhD-Dissertation, Universität Oldenburg 1991.
5.28 J. Lippe and R. Holze, Synth. Met. **41-43** (1991) 2927.
5.29 R. Holze and J. Lippe, Bull. Electrochem. **8** (1992) 516.
5.30 F.J. Dyson, Phys. Rev. **98** (1955) 349.
5.31 R.N. Bagchi, A.M. Bond, and F. Scholz, Electroanalysis **1** (1989) 1.
5.32 W.J. Albery, R.G. Compton, and C.C. Jones, J. Am. Chem. Soc. **106** (1984) 469.
5.33 A.J. Wain, M. Thompson, O.V. Klymenko, and R.G. Compton, Phys. Chem. Chem. Phys. **6** (2004) 4018.
5.34 A.J. Wain and R.G. Compton, J. Electroanal. Chem. **587** (2006) 203.
5.35 A.J. Wain, L. Drouin, and R.G. Compton, J. Electroanal. Chem. **589** (2006) 128.
5.36 A. Petr, L. Dunsch, and A. Neudeck, J. Electroanal. Chem. **412** (1996) 153.
5.37 J. Friedrich and M. Baumgarten, Appl. Magn. Reson. **13** (1997) 393.
5.38 J. Wu, J.B. Day, K. Franaszczuk, B. Montez, E. Oldfield, A. Wieckowski, P.-A. Vuissoz, and J.-P. Ansermet, J. Chem. Soc., Faraday Trans. **93** (1997) 1017.
5.39 J.B. Day, J. Wu, E. Oldfield, and A. Wieckowski in: Electrochemical Nanotechnology (W.J. Lorenz, W. Plieth, Eds.) Wiley-VCH, Weinheim 1998, p. 291.
5.40 Y.Y. Tong, H.S. Kim, P.K. Babu, and A. Wieckowski, J. Am. Chem. Soc. **124** (2002) 468.
5.41 P.K. Babu, Y.Y. Tong, H.S. Kim, and A. Wieckowski, J. Electroanal. Chem. **524-525** (2001) 157.
5.42 P. McGrath, A.M. Fojas, B. Rush, J.A. Reimer, and E.J. Cairns, Electrochemical Society Spring Meeting 209th, Denver, Colorad, USA, May 7-11, 2006, Ext. Abstr. #1097.
5.43 J.B. Wagner Jr. in: Techniques for Characterization of Electrodes and Electrochemical Processes (R. Varma and J.R. Selman Eds.) John Wiley&Sons, New York 1991, p.3